Developmental and Comparative Immunology 128 (2022) 104314

Contents lists available at ScienceDirect

Developmental and Comparative Immunology

journal homepage: www.elsevier.com/locate/devcompimm

Nicotinamide phosphoribosyltransferase (Nampt) of hybrid crucian carp protects intestinal barrier and enhances host immune defense against bacterial infection

Yiyang Tang [a,1], Xiaofeng Liu [b,1], Chen Feng [a], Zejun Zhou [a,*], Shaojun Liu [a,**]

[a] State Key Laboratory of Developmental Biology of Freshwater Fish, College of Life Sciences, Hunan Normal University, Changsha, 410081, China
[b] Department of Nutrition, Xiangya Hospital, Central South University, Changsha, 410008, China

ARTICLE INFO

Keywords:
Hybrid crucian carp
Nicotinamide phosphoribosyltransferase
Antibacterial
Intestinal barrier

ABSTRACT

Nicotinamide phosphoribosyltransferase (Nampt) can act extracellularly as a mediator of inflammation or intracellularly as a rate-limiting enzyme, regulating nicotinamide adenine dinucleotide (NAD) biosynthesis in the NAD salvage pathway. Nampt exerts important immunological functions during infection in mammals. However, the *in vivo* function of fish Nampt in immune regulation and inflammation is essentially unknown. With an aim to elucidate the antimicrobial mechanism of Nampt in fish, we in this study examined the function of Nampt from hybrid crucian carp. Hybrid crucian carp Nampt (WR-Nampt) possesses the conserved nicotinamide phosphoribosyltransferase domain and shows high similarity to that of mammalian Nampt. WR-Nampt is expressed in multiple tissues and is upregulated by bacterial infection. Overexpression of WR-Nampt significantly increased the number of goblet cells of distal intestine. In addition, WR-Nampt induced significant inductions in the expression of the antimicrobial molecules (*IL-22*, *Hepcidin-1*, *LEAP-2* and *MUC2*) and tight junctions (*ZO-1* and *Occludin*). Consistent with this, fish administered with WR-Nampt significantly alleviated the intestinal permeability and apoptosis, thereby enhancing host's resistance against bacterial infection. Together these results revealed the potential effect of WR-Nampt in intestinal barrier and immune defense against bacterial infection.

1. Introduction

Nicotinamide Phosphoribosyltransferase (Nampt), also known as Pre-B-cell colony-enhancing factor (PBEF) or visfatin was found to act as the rate-limiting enzyme in the salvage pathway restoring the cofactor nicotinamide adenine dinucleotide (NAD) (Garten et al., 2015). By controlling NAD production, Nampt can impact on cellular energetics and also on the activity of NAD-dependent enzymes, such as the NADPH oxidase (Sultani et al., 2017). Extracellularly, Nampt was shown to play a prominent role in cell metabolism, inflammation and immune modulation (Travelli et al., 2018). Nampt induces NF-κB transcriptional activities via direct ligation of toll-like receptor 4 (TLR4) (Camp et al., 2015), and extracellular Nampt significantly increases secretion of TNF-α, IL-1β and IL-6 from inflammatory cells (Moschen et al., 2007). In neutrophils, exogenous Nampt delays neutrophil apoptosis and primes neutrophils for the respiratory burst (Jia et al., 2004; Malam et al., 2011). Nampt has been implicated in the pathology of inflammatory diseases (Dakroub et al., 2021; Franco-Trepat et al., 2019). For instance, elevated Nampt levels were described in patients characterized by conditions of acute (respiratory distress syndrome) or chronic (type 2 diabetes, obesity, and cancer) inflammation (Gesing et al., 2017; R Moschen et al., 2010). During infection, inhibition of Nampt enhances the viral growth of cytomegalovirus in both fibroblasts and macrophages, while Nampt activation dramatically inhibits a murine hepatitis virus (MHV) replication (Dantoft et al., 2019; Heer et al., 2020). The ability of Nampt to regulate immune activation, inflammation, together with its role in delaying apoptosis, identifies this protein as an important mediator of inflammatory process.

In intestinal mucosal immunity, the NAD level of intestinal was decreased significantly in *Nampt*$^{-/-}$ mice; histological examination showed that mouse intestinal villi were atrophic and disrupted (Zhang et al., 2017). MUC2, a major component of the mucus layer in the

* Corresponding author. College of Life Science, Hunan Normal University, 36 Lushan Road, Changsha, 410081, China.
** Corresponding authorCollege of Life Science, Hunan Normal University, 36 Lushan Road, Changsha, 410081, China.
E-mail addresses: zhouzejun@hunnu.edu.cn (Z. Zhou), lsj@hunnu.edu.cn (S. Liu).
[1] These authors contributed equally to this work.

https://doi.org/10.1016/j.dci.2021.104314
Received 9 September 2021; Received in revised form 11 November 2021; Accepted 11 November 2021
Available online 14 November 2021
0145-305X/

intestine, is associated with antimicrobial activity and gut immune system function (Holloway et al., 2021). Intriguingly, the MUC2 synthesis was increased by activating enzymes involved in the salvage pathways of NAD^+ biosynthesis in LS 174T goblet cells (Hwang et al., 2018; Ma et al., 2020). Besides, in intestinal disorders such as inflammatory bowel disease (IBD), extracellular Nampt exacerbates the symptoms of colitis, suggesting that extracellular Nampt plays a pro-inflammatory role in IBD (Colombo et al., 2020).

In teleost, Nampt homologue has only been identified in zebrafish. In the early embryonic development of zebrafish, Nampt was widely expressed in brain, fins, intestine and eyes (Fang et al., 2015). Functionally, inhibitors of Nampt caused retinal damage in larval zebrafish (Cassar et al., 2017). In addition, resveratrol reduced the expression of Nampt, resulting in a decrease of NAD^+/NADH ratio in adult zebrafish liver (Schirmer et al., 2012). In a recent paper, Nampt secretion from macrophages was required for muscle regeneration using a zebrafish model (Ratnayake et al., 2021). However, compared to higher vertebrates, very few functional studies about Nampt have been carried out in teleost. As a result, the role of teleost Nampt, especially in immune response and inflammation, is almost unknown.

By using distant hybridization and subsequently selective breeding, hybrid crucian carp (WR, 2n = 100) has been originated from White crucian carp (*Carassius cuvieri*, WCC, female) × Red crucian carp (*Carassius auratus* red var., RCC, male) (Liu et al., 2018). Hybrid crucian carp has many advantages, such as faster growth, better taste and stronger disease resistance compared with their parental species (Liu et al., 2019a; Luo et al., 2021). Currently, hybrid crucian carp has become an economically important species cultured in China (Liu et al., 2019b); however, there are few reports about the immunity of this hybrid crucian carp.

In recent decades, fish motile aeromonad septicemia (MAS) has caused serious economic losses to the Chinese cyprinid fish industry, and *Aeromonas hydrophila* has been identified as the etiologic agent of MAS disease outbreaks (Zhao et al., 2019). *A. hydrophila,* a gram-negative pathogen, has been shown to perturb the integrity of tight junctions in intestinal epithelial cells (Bücker et al., 2011). For example, *A. hydrophila* infection can cause intestinal lesions and inflammation in grass carp (*Ctenopharyngodon idella*) (Kong et al., 2017). In this work, we described the identification of a Nampt homologue from hybrid crucian carp (named WR-Nampt). We found that the expression of WR-Nampt was upregulated by *A. hydrophila* challenge. In addition, we found that WR-Nampt exhibited a protective effect on intestinal barrier, which may provide the first evidence that teleost Nampt is involved in innate immune response against *A. hydrophila* infection.

2. Materials and methods

2.1. Fish

Healthy hybrid crucian carps (average 26 g) were collected from the Engineering Research Center of Polyploid Fish Breeding and Reproduction of State Education Ministry in Hunan Normal University. Hybrid crucian carps (male and female) were randomly collected without gender difference. We followed the laboratory animal guideline for the ethical review of the animal welfare of China (GB/T 35892–2018). Hybrid crucian carps were acclimatized in 70 × 65 × 65 cm plastic aquarium (25 fish/aquarium) and fed with commercial diet twice a day. During the experiment, the water environment was as follows: temperature was 22.01 ± 5.45 °C, pH was 7.1 ± 0.2, and dissolved oxygen was higher than 7.0 mg/L, natural photoperiod, respectively. Before the experiment, fish were randomly sampled and verified to be absent of bacterial pathogens in liver, kidney, blood and spleen as reported previously (Zhou et al., 2020). For tissue collection, fish were euthanized with tricaine methanesulfonate (MS222, Sigma, St. Louis, MO, USA) at a concentration of 100 mg/L.

2.2. Cloning of WR-Nampt

Total RNA was extracted from spleen using Trizol Reagent (Invitrogen, California, CA, USA) as described in the manufacturer's instruction. The first-strand cDNA was synthesized from the previous total RNA using the Maxima H Minus First Strand cDNA Synthesis Kit with dsDNase (Thermo Fisher Scientific, Waltham, MA, USA) according to the manufacturer's protocol. Based on the homologous *Nampt* of teleost, the open reading frame (ORF) of *WR-Nampt* was amplified using primers WR-Nampt-F1/WR-Nampt-R1 (Table S1). The ORF sequence of *WR-Nampt* has been deposited in GenBank database under the accession number OK032063. The DNA template was extracted from spleen by genomic DNA extraction kit (Tiangen biotech, Beijing, China) according to user's manual. After obtaining the cDNA sequence of *WR-Nampt*, the genomic DNA sequence *WR-Nampt* was amplified through primers WR-Nampt-F4/WR-Nampt-R4, WR-Nampt-F5/WR-Nampt-R5, WR-Nampt-F6/WR-Nampt-R6 and WR-Nampt-F7/WR-Nampt-R7 (Table S1).

2.3. Sequence, structure and phylogenetic analysis

The cDNA and amino acid sequences of WR-Nampt were analyzed using the BLAST program at the National Center for Biotechnology Information (NCBI). Domain search was performed with the simple modular architecture research tool (SMART) version 4.0 and the conserved domain search program of NCBI. Multiple sequence alignment was created with Clustal X. Phylogenetic tree was constructed using MEGA4.1 software with the neighbor-joining (NJ) algorithm.

2.4. Quantitative real time reverse transcription-PCR (qRT-PCR)

2.4.1. qRT-PCR analysis of WR-Nampt expression in fish tissues under normal physiological conditions

Liver, spleen, muscle, heart, skin, gill, distal intestine and kidney were taken aseptically from hybrid crucian carps (as described above, five fish in each experiment) and used for total RNA extraction with EZNA Total RNA Kit II (Omega Bio-tek, Doraville, CA, USA). The first-strand cDNA was synthesized as described above. qRT-PCR was carried out in a 7500 Real-time PCR System (Applied Biosystems, Foster City, CA, USA) using the PowerUp SYBR Green Master Mix (Thermo Fisher Scientific). The qRT-PCR program was: 1 cycle of 50 °C/2 min, 1 cycle of 95 °C/2 min, 40 cycles of 95 °C/15 s, 57 °C/15s, 72 °C/35s, followed by dissociation curve analysis (60 °C–95 °C) to verify the amplification of a single product. The expression level of *WR-Nampt* was analyzed using comparative threshold cycle method ($2^{-\Delta\Delta CT}$) with beta-actin (ACTB) as an internal reference (Table S1). PCR efficiency (E) and correlation coefficient (R^2) were conducted as previously described (Zhou et al., 2020). The experiment was performed three times, each time with five fish.

2.4.2. qRT-PCR analysis of WR-Nampt expression in fish tissues during bacterial infection

Aeromonas hydrophila CCL1 (MK014495), a bacterial pathogen isolated from diseased red crucian carps (Zhou et al., 2020), was cultured in Luria-Bertani broth (LB) medium at 28 °C to an OD_{600} of 0.8; the cells were washed with PBS and resuspended in PBS to 1 × 10^5 CFU/mL. Hybrid crucian carps (as described above, five fish in each group) were divided randomly into two groups and injected intramuscularly (i.m.) with 100 μL A. *hydrophila* or PBS (control). Liver, spleen, kidney and distal intestine were taken from the fish (five at each time point) at 0, 6, 12, 24, 36 and 48 h post-bacterial infection. Total RNA extraction, cDNA synthesis, and qRT-PCR were performed as described above. The experiment was performed three times.

2.5. Construction of pWR-Nampt

To construct the eukaryotic expression plasmid pWR-Nampt, which

expresses His-tagged WR-Nampt, the coding sequence of WR-Nampt was amplified with primers WR-Nampt-F3 and WR-Nampt-R3, and the PCR products were inserted into the eukaryotic expression vector pCN3 (Zhou and Sun, 2016) at the EcoRV site. After that, endotoxin-free plasmids (pWR-Nampt and pCN3) were prepared using Endo-Free plasmid Kit (Omega Bio-Tek). The quality of the DNA was examined by determining A260/280 and A260/230 absorbance ratio using NanoDrop 2000 (Thermo Fisher Scientific) and by gel electrophoresis. pWR-Nampt and pCN3 were diluted in PBS to 200 μg/mL based on previous and preliminary experiment (Feng et al., 2021).

2.6. In vivo effect of pWR-Nampt overexpression on intestinal barrier function

Hybrid crucian carps (as above, three fish in each group) were divided randomly into three groups and injected i.m. with 100 μL of pWR-Nampt, pCN3, or PBS (control). Distal intestine was taken from the fish at 3 d post-plasmid administration and used for examination of the presence of plasmids and WR-Nampt expression. For plasmid detection, DNA was extracted from the tissues with the TIANamp DNA Kit (Tiangen). PCR detection of pCN3 was performed with the primers CN–F1 and CN-R1; PCR detection of pWR-Nampt was performed with the primers CN–F1 and WR-Nampt-R3. To examine expression of plasmid-derived WR-Nampt, total RNA was extracted from the tissues and used for qRT-PCR with the primers WR-Nampt-F3 and His-R. As an internal control, qRT-PCR was also performed with the primers specific to beta-actin (Table S1).

At 3 days post-plasmid administration as above, the fish (three fish in each group) were infected via i.m. injection with *A. hydrophila* CCL1 (1×10^4 CFU/fish). At 24 h post-infection (hpi), distal intestine from pWR-Nampt, pCN3, or PBS (control) injected fish was taken under aseptic conditions and total RNA was prepared as described above. qRT-PCR was used to analyze the expression of *IL-22*, *MUC2*, *Hepcidin-1*, *LEAP-2*, *ZO-1*, *Occludin*, *Claudin-1*, *Claudin-2*, *Claudin-4*, *Claudin-8*, *IL-1β* and *TNF-α* as above. The PCR primers are listed in Table S1. The transcripts were sequenced to confirm the specificity (Fig. S1). The experiment was performed three times, each time with five fish. The results showed that the PCR efficiencies ranged from 90% to 108%, and the correlation coefficients ranged from 0.990 to 0.998 (data not shown).

At 24 hpi of *A. hydrophila*, plasma was prepared from the blood of pWR-Nampt, pCN3, or PBS (control) injected fish (three fish in each group). The plasma LPS, a representative biological marker of mucosal permeability, was then quantified using limulus amebocyte lysate QCL-1000 kit as descripted in our previous study (Zhou et al., 2018). To measure the number of goblet cells (GCs), at 24 hpi of *A. hydrophila*, the distal intestine from pWR-Nampt, pCN3, or PBS (control) injected fish was immediately transferred to 4% paraformaldehyde solution for alcian blue/periodic acid-Schiff (AB-PAS) Staining Kit (Solarbio) as reported previously (Feng et al., 2021). The goblet cells (dark blue dots) per a villus in each section were counted in three to four fields of view using a light microscope. The experiment was performed three times, each time with three replicates.

2.7. In vivo effect of pWR-Nampt overexpression on NAD^+/NADH levels

At 3 days post-plasmid administration as above, the fish (three fish in each group) were infected via i.m. injection with *A. hydrophila* CCL1 (1×10^4 CFU/fish). At 24 hpi, 30 mg distal intestine samples were taken and washed with pre-cooled PBS on ice. The NAD^+/NADH levels were then detected by NAD^+/NADH Assay Kit (Beyotime, Shanghai, China) as described in the manufacturer's instruction. Briefly, the sample was placed in a homogenizer, and 400 μL NAD^+/NADH extract buffer was added for homogenization on ice. The supernatant were collected by centrifugation at 12,000g, 4 °C, 10 min, and then were treated with or without heat treatment at 60 °C for 30 min 90 μL ethanol working solution were added into the samples. After incubation at 37 °C for 30 min, 10 μL WST-8 chromogenic buffer were added and the plate was read at 450 nm with a microplate reader. The experiment was performed three times, each time with three replicates.

2.8. In vivo effect of pWR-Nampt overexpression on apoptosis of intestinal epithelium cells

At 3 days post-plasmid administration as above, the fish (three fish in each group) were infected via i.m. injection with *A. hydrophila* CCL1 (1×10^4 CFU/fish). At 24 hpi, distal intestine were fixed in 4% paraformaldehyde at room temperature for 24 h, and faded in 70% ethanol 2 h for 4 times, and dehydrated in 80%, 95% and 100% ethanol sequentially. Then the samples were embedded in paraffin wax, sectioned (6 μm) and mounted on slides. The slides were deparaffinated in xylene, rehydrated in diluted ethanol series from 95% up to distilled water. Antigen retrieval was performed by high-pressure steam method using the commercially available citrate antigen retrieval solution (Sangon Biotech., Shanghai, China). Briefly, the slides were immersed in a coplin jar filled with diluted target retrieval solution. The coplin jar was then placed in a pressure cooker for 6 min at 15 psi (121 °C). The slides were washed three times with PBS after the retrieval solution is cooled to room temperature. The slides were then blocked with 3% BSA in PBS at 37 °C for 30 min. Mouse *anti*-E-cadherin antibody (13–5700, Thermo Fisher Scientific, diluted 1:500 in 3% BSA) and rabbit anti-active Caspase 3 antibody (MA5-32015, Thermo Fisher Scientific, diluted 1:500 in 3% BSA) were added to the slide. The slide was incubated at 4 °C for overnight and washed in PBS containing 0.1% Tween-20 (PBS-T) for three times. Cy3-conjugated goat anti-mouse IgG antibody (Sangon Biotech., D110088, 1/500 dilution) and Alexa Fluor 488-conjugated goat anti-rabbit IgG antibody (Sangon Biotech., D110061, 1/500 dilution) in PBS containing 3% BSA were added to the slide. The slide was incubated at 37 °C for 1 h. After washing with PBS-T for three times, sections were incubated with DAPI (Sangon Biotech., E607303) for 5 min. Finally, the sections were washed with PBS-T and observed with a fluorescence microscopy (Olympus DP73, Tokyo, Japan). The experiment was performed three times.

2.9. In vivo effect of pWR-Nampt overexpression on A. hydrophila infection

At 3 days post-plasmid administration as above, the fish (three fish in each group) were infected via i.m. injection with *A. hydrophila* (1×10^4 CFU/fish). At 24 and 48 hpi, kidney and spleen were taken under aseptic conditions and examined for bacterial numbers by plate count as reported previously (Zhou and Sun, 2015). The experiment was performed three times, each time with three replicates. To calculate the survival percentage, fish with or without pWR-Nampt overexpression (twenty fish in each group) were infected with *A. hydrophila* as above, and fish mortality during infection was recorded and calculated in three weeks.

2.10. Statistical analysis

All experiments were performed in triplicate or independently for three times, and statistical analyses were carried out with GraphPad Prism 6 (GraphPad Software, San Diego, CA, USA). Data were analyzed with one-way analysis of variance (ANOVA) with Kruskal-Wallis' comparison or 2-way ANOVA with Tukey's comparison, and statistical significance was defined as $P < 0.05$. For statistical analysis in the survival experiment, log-rank test was used. For the qRT-PCR, the relative expressions are normalized via β-actin expression before calculating the relative expression levels to PBS/0 h treatment.

3. Results

3.1. Sequence characteristics of WR-Nampt

The deduced amino acid sequence of WR-Nampt is composed of 556 residues, which has a calculated molecular mass of 62.7 kDa and a pI of 6.8. *In silico* analysis identified a conserved nicotinamide phosphoribosyltransferase domain in WR-Nampt (Fig. 1). Sequence alignment showed that WR-Nampt shares 82.9%–90.6% overall sequence identities with the teleost species including large yellow croaker, tilapia,

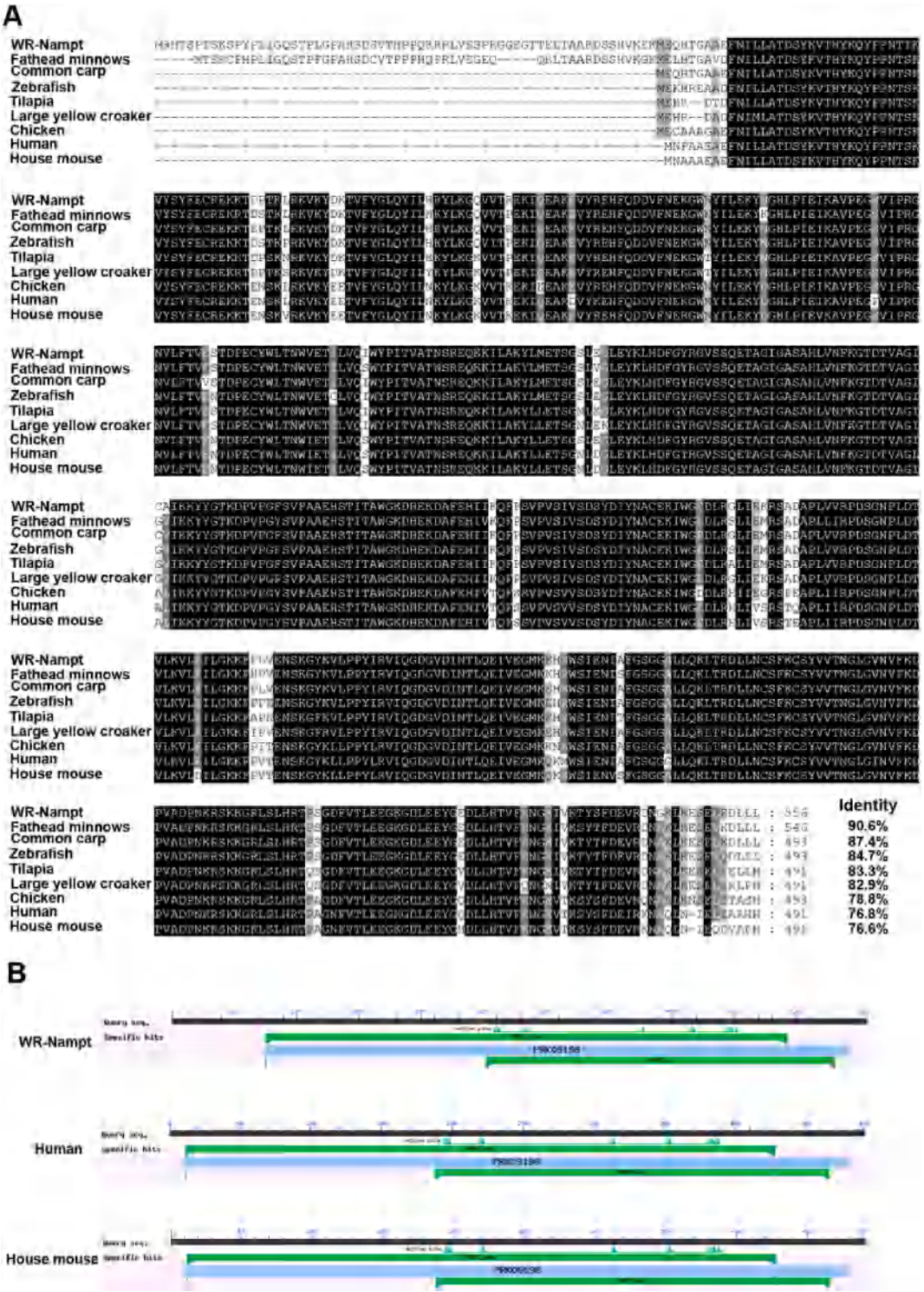

Fig. 1. Sequence and structure of WR-Nampt. (A) Alignment of the sequences of WR-Nampt homologues. Dots denote gaps introduced for maximum matching. Numbers in the end of each line indicate overall sequence identities between WR-Nampt and the compared sequences. The consensus residues are in black, the residues that are ≥90% identical among the aligned sequences are in grey. The GenBank accession numbers of the aligned sequences are as follows: WR-Nampt, OK032063; Fathead minnows, XP_039516638.1; Common carp, XP_018936796.1; Zebrafish, XP_002661386.1; Tilapia, XP_003450758.3; Large yellow croaker, NP_001290284.1; Chicken, NP_001025899.1; Human, NP_005737.1; House mouse, NP_067499.2. (B) Nicotinamide phosphoribosyltransferase domain of WR-Nampt, human and house mouse Nampt. (For interpretation of the references to colour in this figure legend, the reader is referred to the Web version of this article.)

zebrafish, common carp and fathead minnows. The overall sequence identity between WR-Nampt and human and house mouse WR-Nampt are 76.8% and 76.6%, respectively (Fig. 1).

The genomic sequence of *WR-Nampt* possessed eleven exons, which is the same in zebrafish, tropical clawed frog, common wall lizard, house mouse and human (Fig. 2A). In addition, the amino acid sequences of WR-Nampt and other Nampt from different vertebrates were collected to construct the phylogenetic tree using neighbor joining algorithm based on multiple sequence alignment. The WR-Nampt firstly clusters with WR-Nampt from common carp, and then clusters with the same molecules from other teleost, suggesting a close relationship of WR-Nampt with its homologs from teleost (Fig. 2B). The Nampt from other vertebrates, such as amphibian, reptile, avian and mammal, form sister groups of the group formed by teleost Nampt (Fig. 2B).

3.2. *WR-Nampt expression in the absence and presence of A. hydrophila infection*

qRT-PCR analysis showed that under normal physiological conditions, WR-Nampt expression was detected, in increasing order, in the liver, spleen, muscle, heart, skin, gill, distal intestine and kidney of hybrid crucian carp (Fig. 3A–B). When the fish were infected with the bacterial pathogen *A. hydrophila*, significant inductions of WR-Nampt expression were detected in spleen and liver at 6 and 12 hpi, with the highest level of induction occurring at 12 hpi (Fig. 4C-D). In kidney and intestine, *A. hydrophila* infection induced WR-Nampt expression to significant levels at 12, 24 and 36 hpi, with the highest level of induction occurring at 24 hpi (Fig. 4A-B).

3.3. *Effect of WR-Nampt on intestine goblet cells*

To examine whether WR-Nampt has any *in vivo* effect with respect to

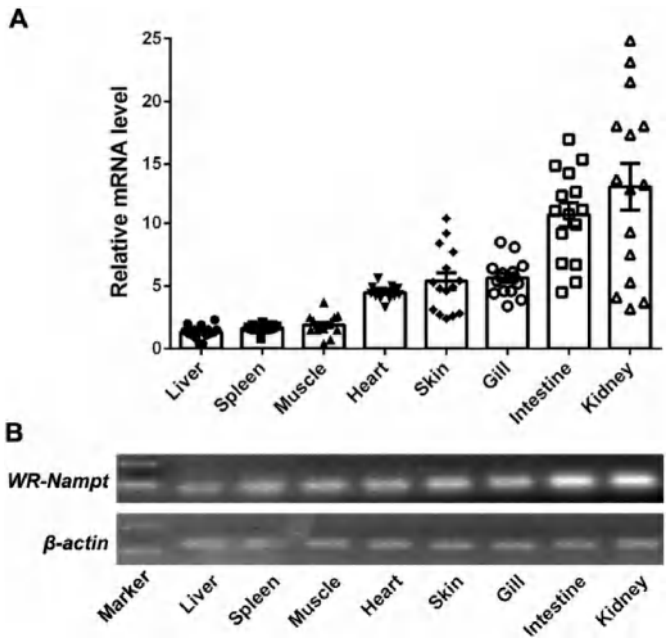

Fig. 3. WR-Nampt expression in fish tissues under normal physiological condition. (A) WR-Nampt expression in the liver, spleen, muscle, heart, skin, gill, distal intestine and kidney of hybrid crucian carp was determined by quantitative real time RT-PCR. For convenience of comparison, the expression level in liver was set as 1. (B) WR-Nampt expression in above fish tissues was determined by RT-PCR. Values are shown as means ± SEM (N = 3). N, the number of times the experiment was performed.

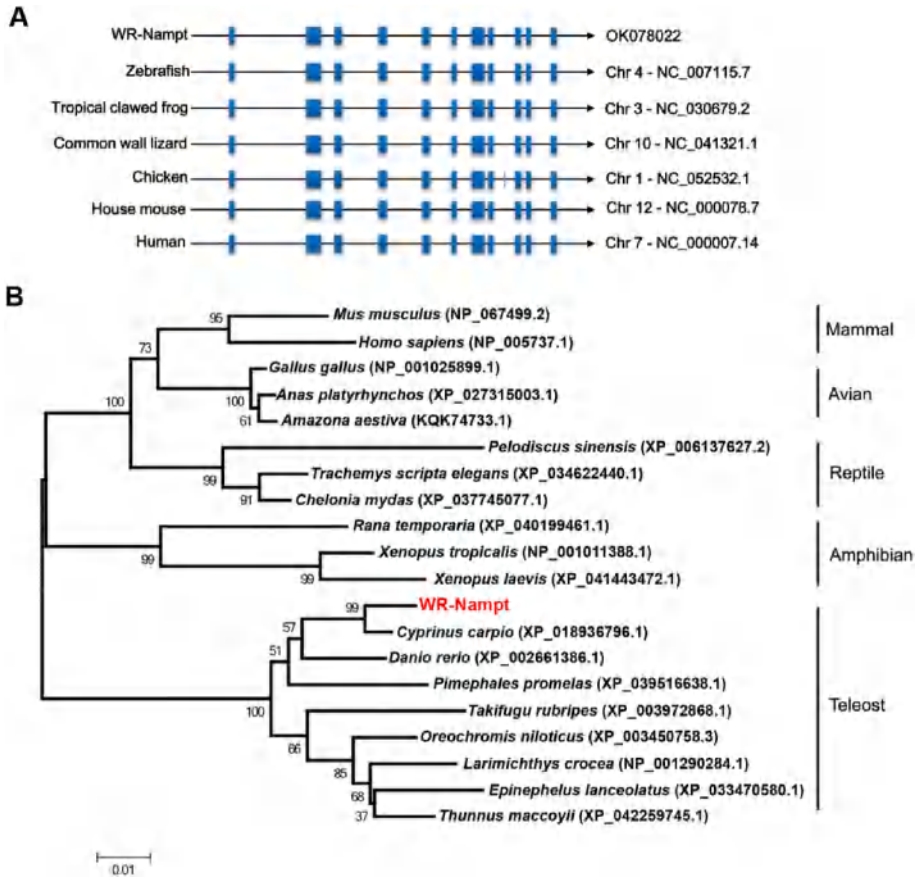

Fig. 2. Evolutionary conservation of WR-Nampt. (A) Genomic structures of WR-Nampt and other vertebrates. Rectangles represent coding exons. The horizontal lines between two rectangles represent introns. (B) Phylogenetic trees constructed with the amino acid sequences of Nampt from the indicated species. The tree was constructed using the neighbor-joining (NJ) algorithm with the Mega 4.1 program based on multiple sequence alignment by Clustal X. Bootstrap values of 1000 replicates (%) are indicated for the branches.

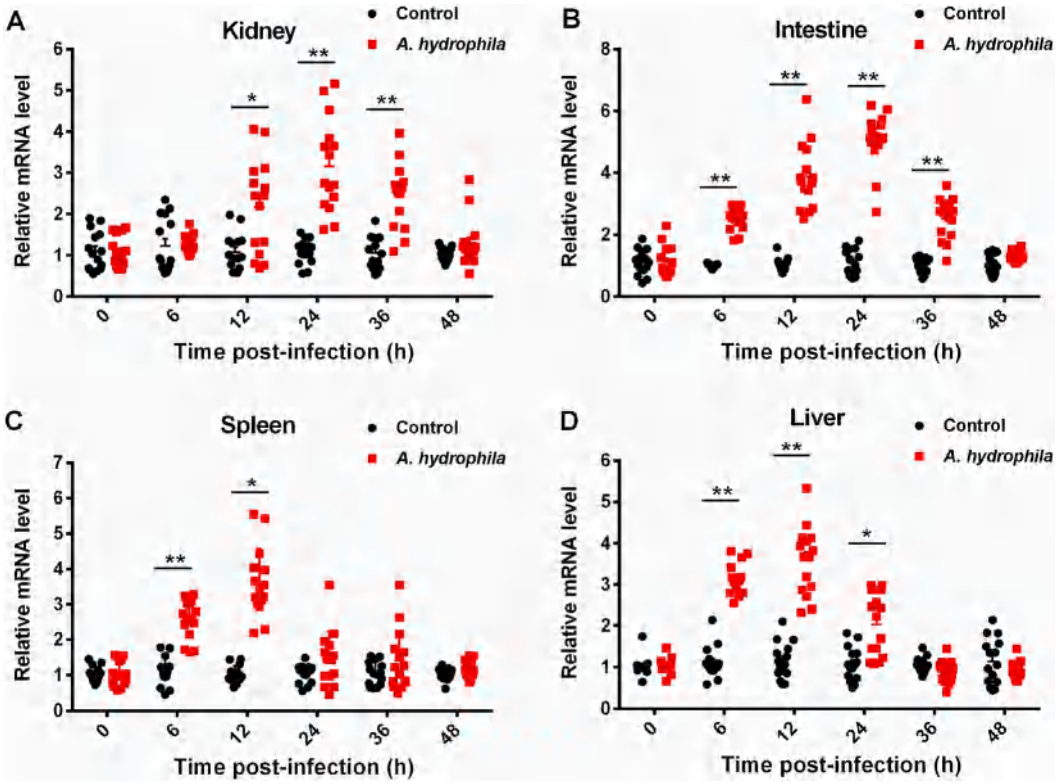

Fig. 4. WR-Nampt expression during bacterial infection. Hybrid crucian carps were infected with or without (control) *Aeromonas hydrophila*, and WR-Nampt expression in kidney (A), distal intestine (B), spleen (C) and liver (D) were determined by quantitative real time RT-PCR at various time points. In each case, the expression level of the control fish was set as 1. Values are shown as means ± SEM (N = 3). N, the number of times the experiment was performed. $^{*}P < 0.05$, $^{**}P < 0.01$.

immune defense against pathogen invasion, hybrid crucian carps were pre-administered with pWR-Nampt, pCN3, or PBS (control). PCR analysis showed that pWR-Nampt and pCN3 were present in the intestine of the fish administered with the respective plasmids but not in the fish administered with PBS (Fig. S2), while qRT-PCR showed that mRNA specific to plasmid-encoded WR-Nampt was present in the intestine of the fish administered with pWR-Nampt, but not in the fish administered with pCN3 or PBS (Fig. S2).

Goblet cells (GCs) are responsible for coating the intestinal epithelium with a protective layer of mucus, and thus, we compared the number of GCs during *A. hydrophila* infection by AB-PAS staining. The results showed that compared to the fish administered with pWR-Nampt, GC numbers in PBS or pCN3 administered fish were significantly decreased (Fig. 5A–B). Further, qRT-PCR analysis showed that compared to treatment with PBS or pCN3, treatment of fish with pWR-Nampt induced significant inductions in the expression of *IL-22*, *Hepcidin-1*, *LEAP-2* and *MUC2* (Fig. 5C–F).

3.4. Effect of WR-Nampt on intestine barrier function

NAD^+, which is the core cofactor of mitochondrial function, plays a vital role in regulating cell metabolism and energy homeostasis (Garten et al., 2015). We found that the NAD^+/NADH level was significantly increased in the fish administered with pWR-Nampt compared that in pCN3 or PBS administered fish (Fig. 6A). Plasma LPS, which is translocated from dysfunctional mucosal barriers, has been considered to a representative biological marker of mucosal permeability (Ogunrinde et al., 2019). For this purpose, we measured the plasma LPS levels in the fish administered with pWR-Nampt, pCN3, or PBS (control) during pathogen infection. The results showed that the plasma LPS level in the fish administered with pWR-Nampt was significantly decreased compared that in pCN3 or PBS administered fish (Fig. 6B). Immunohistochemistry assay was performed to further characterize the protection of pWR-Nampt on intestinal epithelium cells. The results showed that compared to that in PBS or pCN3 administered fish, the apoptosis of epithelial cells was significantly inhibited in the fish administered with pWR-Nampt (Fig. 6C). qRT-PCR analysis showed that in the fish administered with pWR-Nampt, the expression of *ZO-1* and *Occludin*, but not *Claudin-1, -2, -4* and *-8*, in intestine were significantly increased compared to the control fish (Fig. 6D–I). In contrast, administered with pCN3 or PBS had no apparent effect on the expression of these genes.

3.5. Effect of WR-Nampt overexpression on bacterial infection

To further verify our finding, the fish pre-administered with pWR-Nampt, pCN3, or PBS (control) were challenged with *A. hydrophila*, and bacterial loads in the kidney and spleen of the fish were determined. The results showed that the bacterial numbers were significantly reduced in pWR-Nampt treated fish, whereas the bacterial numbers in pCN3 treated fish were comparable to those in the control fish treated with PBS (Fig. 7A and B). In addition, qRT-PCR analysis showed that in the fish administered with pWR-Nampt, the expression of *IL-1β* and *TNF-α* were significantly increased compared to the control fish (Fig. 7C and D). In contrast, administered with pCN3 had no apparent effect on the expression of these genes. Correlated with that, the fish administered with pWR-Nampt have higher survival rate than the PBS or pCN3 administered fish within 21 days (Fig. 7E).

4. Discussion

Nampt, also known as PBEF and visfatin, can act intracellularly regulating NAD biosynthesis in the NAD salvage pathway (Sultani et al., 2017). Extracellularly, Nampt has been shown to stimulate expression of

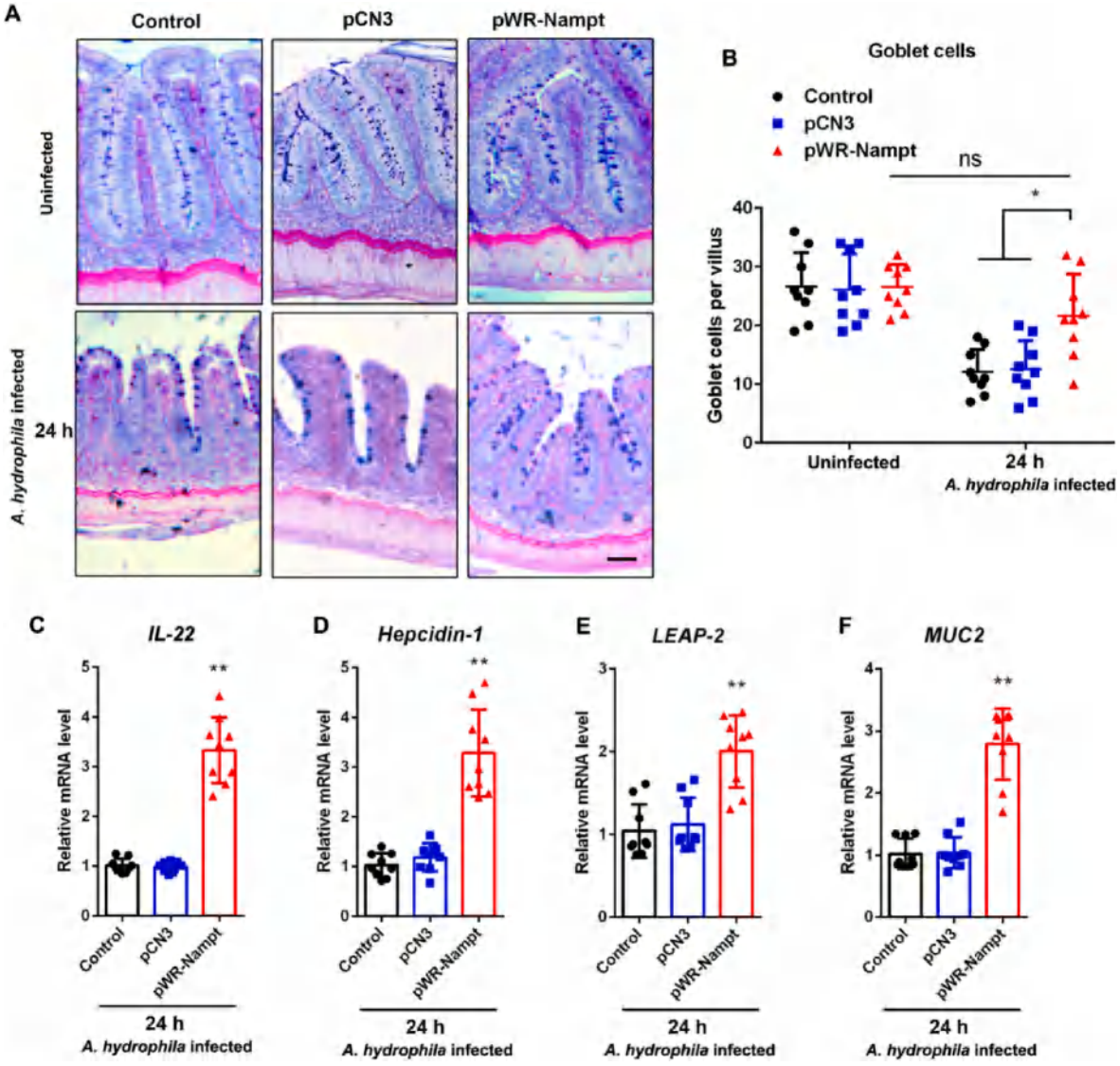

Fig. 5. WR-Nampt increases intestinal goblet cells. (A–F) Hybrid crucian carps were administered with pWR-Nampt, pCN3 or PBS. At 3 days post-plasmid administration, carps were infected with *Aeromonas hydrophila* for 24 h. (A and B) The goblet cells (GCs) numbers of distal intestine from pWR-Nampt, pCN3, or PBS (control) injected fish were measured by AB-PAS staining. Bar: 50 μm. (C–F) Relative mRNA levels of the indicated molecules in intestine were analyzed by quantitative real-time RT-PCR. Values are shown as means ± SEM (N = 3). N, the number of times the experiment was performed. $^{*}P < 0.05$, $^{**}P < 0.01$. Ns: no significance.

cytokines, matrix-degrading enzymes, and chemokines in monocytes (Travelli et al., 2018). In neutrophils, exogenous Nampt delays neutrophil apoptosis and primes neutrophils for the respiratory burst (Jia et al., 2004; Malam et al., 2011). Nevertheless, most studies related to Nampt are focusing on higher vertebrates, especially the mammals, whether and how the Nampt controls immune responses in early vertebrates remains largely unknown. In the present work, we cloned the sequence of Nampt in hybrid crucian carp (WR-Nampt). SMART analysis showed that the WR-Nampt is a highly conserved nicotinamide phosphoribosyltransferase, and shares highly similarity of structure with its mammalian homologues. The results of blast and phylogenetic analysis showed that WR-Nampt is a highly conserved molecule from fish to mammals, indicating that it may perform similar functions to higher vertebrates.

In mammals, Nampt has a ubiquitous expression in several cells, tissues and organs (Chen et al., 2007). In the early embryo development of zebrafish, Nampt was widely expressed across many tissues, including brain, fins, intestine and eyes (Fang et al., 2015). In our study, WR-Nampt expression was found to be relatively high in kidney and intestine, moderate in gill, skin and heart, and low in muscle, spleen and liver. Further study is remained to illustrate this tissue-specific expression pattern and its internal mechanisms. In human, elevated Nampt levels in obese children were mainly derived from leucocytes and inducible by lipopolysaccharide (LPS) (Friebe et al., 2011). Nampt levels were also selectively elevated in acute infectious disease and in acute relapse of chronic inflammatory diseases in children (Gesing et al., 2017). Furthermore, recent study has shown that Nampt was up-regulated in SARS-CoV-2-infected cells and may play a positive antiviral activity (Heer et al., 2020). In this study, experimental infection with a bacterial pathogen caused significant induction of WR-Nampt expression in kidney, intestine, liver and spleen. As we know, consist with mammals, kidney, intestine, liver and spleen are generally considered as immune organs and the center of immune responses in teleost, because a large number of immune cells colonize in these organs and participate in immune response during pathogen invasion. These observations suggested a possible universal role of fish Nampt in pathogen infection and host immune defense.

Goblet cells (GCs) secrete protective mucins that are required for the

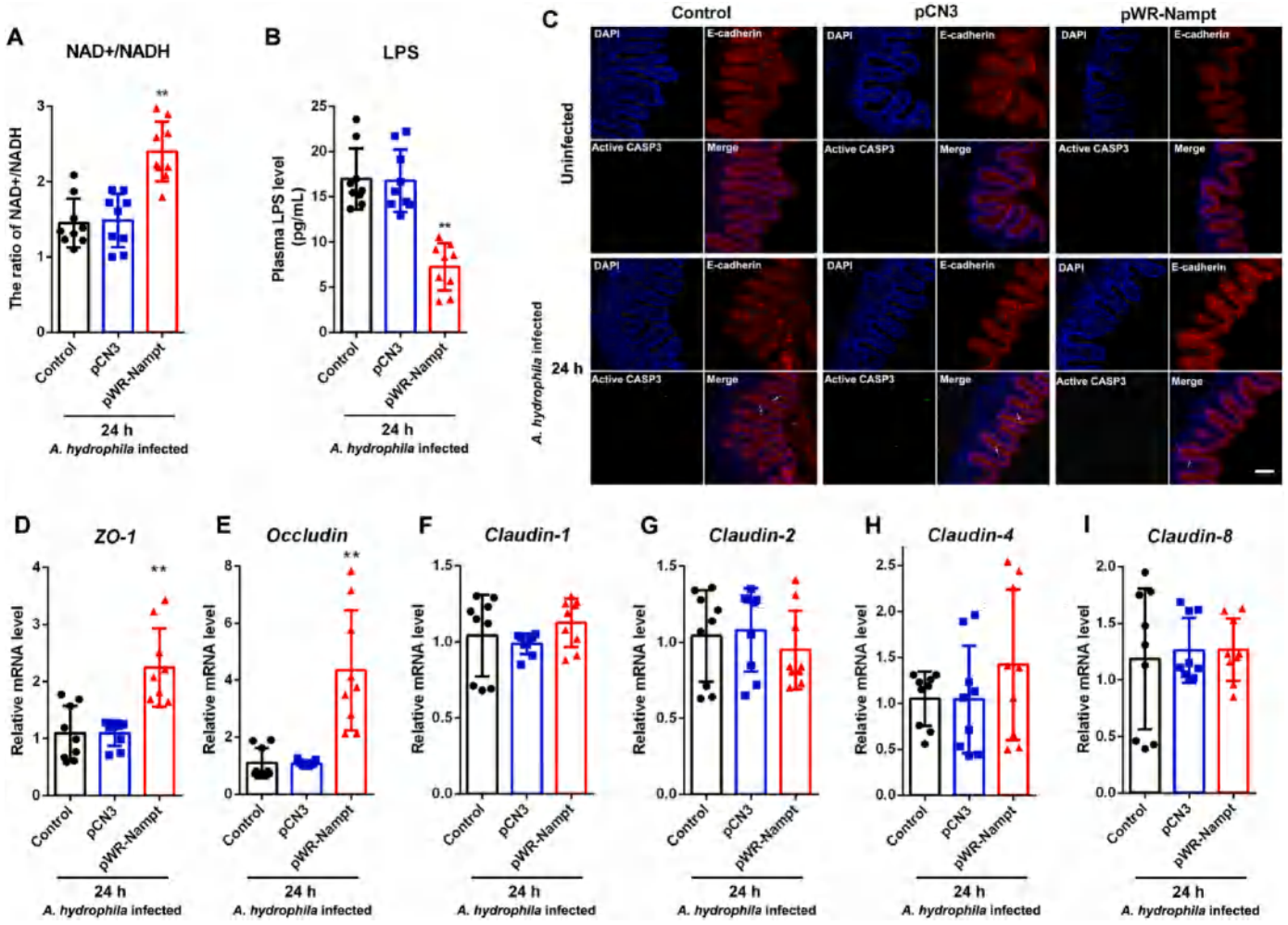

Fig. 6. WR-Nampt protects intestinal barrier. (A–I) Hybrid crucian carps were administered with pWR-Nampt, pCN3 or PBS. At 3 days post-plasmid administration, carps were infected with *Aeromonas hydrophila* for 24 h. (A) The NAD^+/NADH levels were detected by NAD^+/NADH Assay Kit. (B) Plasma LPS levels in the fish were determined by limulus amebocyte lysate QCL-1000 kit. (C) Apoptosis of intestinal epithelium cells were determined by immunohistochemistry analysis. Bar: 50 μm. (D–I) The expressions of tight junction relevant genes in distal intestine were determined by quantitative real time RT-PCR. For convenience of comparison, the expression levels of PBS treatment were set as 1. Values are shown as means ± SEM (N = 3). N, the number of times the experiment was performed. $^{**}P < 0.01$.

movement and effective expulsion of gut contents, and provide protection against pathogen infection (Gehart and Clevers, 2019). When sentinel goblet cells detect bacterial invasion via toll-like receptors they secrete the mucus protein mucin 2 (MUC2) and are associated with antimicrobial activity and gut immune system function (Holloway et al., 2021). Intriguingly, previous studies have shown that enhanced NAD^+ levels stimulate MUC2 expression in human goblet cells (Hwang et al., 2018; Ma et al., 2020). In line with this, we found that the numbers of GCs and *MUC2* expression were significantly increased in pWR-Nampt administered fish, suggesting WR-Nampt may protect intestinal goblet cells during bacterial invasion. IL-22 plays a critical role in the maintenance and defense of the gut epithelial barrier, including inducing the release of antimicrobial peptides, increasing the number of goblet cells and the expression of MUC2 (Sugimoto et al., 2008). In contrast, depletion of NAD^+ levels suppressed the production of IL-22 in mouse (Gardner et al., 2013). In our study, we found the expression of *IL-22* and the antimicrobial molecules (*MUC2*, *Hepcidin-1* and *LEAP-2*) were significantly increased in the pWR-Nampt administered fish, which suggest a possible involvement of WR-Nampt in intestinal barrier against microbial pathogens.

Tight junctions are essential for establishing a barrier in epithelial tissues (Zihni et al., 2016). Tight junctions can be disrupted by invading pathogens, which may result in increased mucosal permeability and subsequent systemic inflammation (Luo et al., 2019). Previous studies have showed that NAD^+ ameliorates inflammation-induced epithelial barrier dysfunction in cultured enterocytes and mouse ileal mucosa (Han et al., 2003). In contrast, inhibition of Nampt induces apoptosis and detachment of epithelial cells, leading to the dysfunction of mucosa barrier (Li et al., 2019). In the present study, we found that the NAD^+/NADH level was significantly increased in the pWR-Nampt-administered fish. Additionally, LPS, a representative biological marker of intestinal permeability, was significantly reduced in pWR-Nampt treated fish. Moreover, pWR-Nampt induced a significant expression of *ZO-1* and *Occludin*. These results indicate that WR-Nampt may prevent pathogens invasion by enhancing the intestinal barrier and thus play a protective role in the immune defense during bacterial infection. However, another possibility is that the decrease in LPS levels is due to some direct bactericidal mechanisms of WR-Nampt, which leads to a reduced load of *A. hydrophila* in circulation. Inhibition of the NAD^+ biosynthesis resulted in an increased mucosal destruction and cecal hemorrhage in response to *Clostridium difficile* infection (El-Zaatari et al., 2014). In our study, when the fish were infected with *A. hydrophila*, the bacterial loads in the tissues of pWR-Nampt-administered fish were significantly lower than those in the control group. And the expression of *IL-1β* and *TNF-α* were also significantly increased in pWR-Nampt-administered fish. Taken together, these results suggest

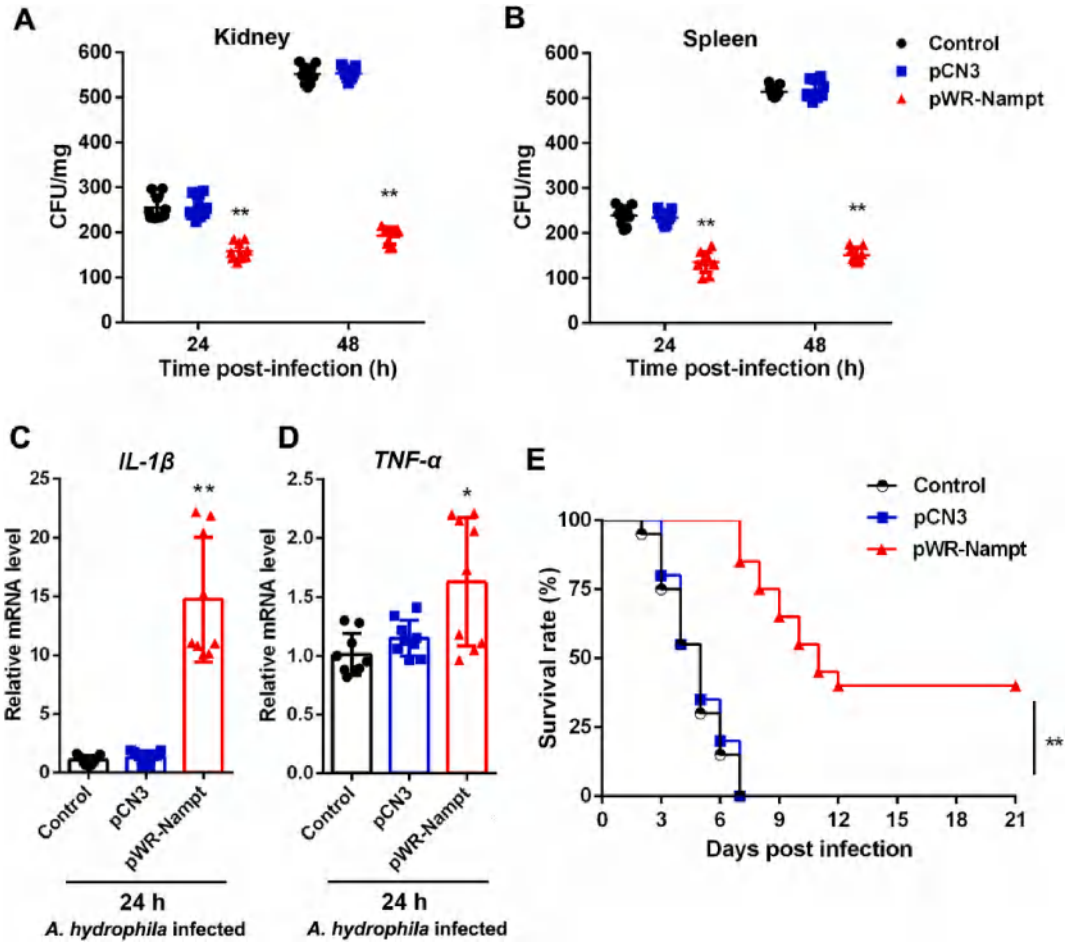

Fig. 7. Effect of WR-Nampt overexpression on bacterial infection. (A–E) Hybrid crucian carps were administered with pWR-Nampt, pCN3, or PBS (control). At 3 days post-plasmid administration, carps were infected with *Aeromonas hydrophila* for 24 h. The fish pre-administered with pWR-Nampt, pCN3, or PBS (control) were challenged with *A. hydrophila*, and bacterial loads in the kidney (A) and spleen (B) of the fish were determined at different time points. (C and D) The expression of the *IL-1β* and *TNF-α* was then determined by quantitative real time RT-PCR. For convenience of comparison, the expression levels of PBS treatment were set as 1. (E) The fish pre-administered with pWR-Nampt, pCN3, or PBS (control) were challenged with *A. hydrophila*, and the survival rates were recorded in three weeks. Significant difference was determined with a log-rank test (**$P < 0.01$). Values are shown as means ± SEM (N = 3). N, the number of times the experiment was performed. *$P < 0.05$, **$P < 0.01$.

that pWR-Nampt may effectively protect hybrid crucian carp from *A. hydrophila* infection by limiting bacterial colonization *in vivo* through some direct or indirect antimicrobial mechanisms (i.e. induction of cytokines).

In conclusion, this study demonstrates that WR-Nampt, as a highly conserved nicotinamide phosphoribosyltransferase, is upregulated in expression by bacterial infection. WR-Nampt exhibits a significant protective effect on intestinal barrier and restricts the colonization of *A. hydrophila* in systemic immune organs. These results provide us a new insight into the immune mechanism of teleost Nampt in antibacterial immunity *in vivo*. In the future, we will try to express the recombinant WR-Nampt protein and determine its enzyme activity *in vitro*. In addition, we will prepare its polyclonal or monoclonal antibody, and verify whether fish Nampt has the same function as mammals.

Acknowledgements

This research was supported by the National Natural Science Foundation of China (32102847), Natural Science Foundation of Hunan Province (2020JJ5360), Changsha Municipal Natural Science Foundation (kq2014277), Scientific Research Foundation of Hunan Provincial Education Department (19B366), High Level Talent Agglomeration Program of Hunan, China (2019RS1044), 111 Project (D20007) and Research Startup Project of Hunan Normal University (0531120–3675).

Appendix A. Supplementary data

Supplementary data to this article can be found online at https://doi.org/10.1016/j.dci.2021.104314.

References

Bücker, R., Krug, S.M., Rosenthal, R., Günzel, D., Fromm, A., Zeitz, M., Chakraborty, T., Fromm, M., Epple, H.J., Schulzke, J.D., 2011. Aerolysin from *Aeromonas hydrophila* perturbs tight junction integrity and cell lesion repair in intestinal epithelial HT-29/B6 cells. J. Infect. Dis. 204, 1283–1292.

Camp, S.M., Ceco, E., Evenoski, C.L., Danilov, S.M., Zhou, T., Chiang, E.T., Moreno-Vinasco, L., Mapes, B., Zhao, J., Gursoy, G., Brown, M.E., Adyshev, D.M., Siddiqui, S. S., Quijada, H., Sammani, S., Letsiou, E., Saadat, L., Yousef, M., Wang, T., Liang, J., Garcia, J.G., 2015. Unique toll-like receptor 4 activation by NAMPT/PBEF induces NFκB signaling and inflammatory lung injury. Sci. Rep. 5, 13135.

Cassar, S., Dunn, C., Olson, A., Buck, W., Fossey, S., Ramos, M.F., Sancheti, P., Stolarik, D., Britton, H., Cole, T., Bratcher, N., Huang, X., Peterson, R., Longenecker, K., LeRoy, B., 2017. Inhibitors of nicotinamide phosphoribosyltransferase cause retinal damage in larval zebrafish. Toxicol. Sci. 161, 300–309.

Colombo, G., Clemente, N., Zito, A., Bracci, C., Colombo, F.S., Sangaletti, S., Jachetti, E., Ribaldone, D.G., Caviglia, G.P., Pastorelli, L., De Andrea, M., Naviglio, S., Lucafò, M., Stocco, G., Grolla, A.A., Campolo, M., Casili, G., Cuzzocrea, S., Esposito, E., Malavasi, F., Genazzani, A.A., Porta, C., Travelli, C., 2020. Neutralization of

extracellular NAMPT (nicotinamide phosphoribosyltransferase) ameliorates experimental murine colitis. J. Mol. Med. 98, 595–612.
Chen, H., Xia, T., Zhou, L., Chen, X., Gan, L., Yao, W., Peng, Y., Yang, Z., 2007. Gene organization, alternate splicing and expression pattern of porcine visfatin gene. Domest. Anim. Endocrinol. 32, 235–245.
Dakroub, A., Nasser, S.A., Kobeissy, F., 2021. Visfatin: an emerging adipocytokine bridging the gap in the evolution of cardiovascular diseases. J. Cell. Physiol. 236, 6282–6296.
Dantoft, W., Robertson, K.A., Watkins, W.J., Strobl, B., Ghazal, P., 2019. Metabolic regulators Nampt and Sirt6 serially participate in the macrophage interferon antiviral cascade. Front. Microbiol. 10, 355.
El-Zaatari, M., Chang, Y.M., Zhang, M., Franz, M., Shreiner, A., McDermott, A.J., van der Sluijs, K.F., Lutter, R., Grasberger, H., Kamada, N., Young, V.B., Huffnagle, G.B., Kao, J.Y., 2014. Tryptophan catabolism restricts IFN-γ-expressing neutrophils and *Clostridium difficile* immunopathology. J. Immunol. 193, 807–816.
Fang, C., Guan, L., Zhong, Z., Gan, X., He, S., 2015. Analysis of the nicotinamide phosphoribosyltransferase family provides insight into vertebrate adaptation to different oxygen levels during the water-to-land transition. FEBS J. 282, 2858–2878.
Feng, C., Tang, Y., Liu, X., Zhou, Z., 2021. CMPK2 of triploid crucian carp is involved in immune defense against bacterial infection. Dev. Comp. Immunol. 116, 103924.
Franco-Trepat, E., Alonso-Pérez, A., Guillán-Fresco, M., Jorge-Mora, A., Gualillo, O., Gómez-Reino, J.J., Gómez Bahamonde, R., 2019. Visfatin as a therapeutic target for rheumatoid arthritis. Expert Opin. Ther. Targets 23, 607–618.
Friebe, D., Neef, M., Kratzsch, J., Erbs, S., Dittrich, K., Garten, A., Petzold-Quinque, S., Blüher, S., Reinehr, T., Stumvoll, M., Blüher, M., Kiess, W., Körner, A., 2011. Leucocytes are a major source of circulating nicotinamide phosphoribosyltransferase (NAMPT)/pre-B cell colony (PBEF)/visfatin linking obesity and inflammation in humans. Diabetologia 54, 1200–1211.
Gardner, P.J., Joshi, L., Lee, R.W., Dick, A.D., Adamson, P., Calder, V.L., 2013. SIRT1 activation protects against autoimmune T cell-driven retinal disease in mice via inhibition of IL-2/Stat5 signaling. J. Autoimmun. 42, 117–129.
Garten, A., Schuster, S., Penke, M., Gorski, T., de Giorgis, T., Kiess, W., 2015. Physiological and pathophysiological roles of NAMPT and NAD metabolism. Nat. Rev. Endocrinol. 11, 535–546.
Gehart, H., Clevers, H., 2019. Tales from the crypt: new insights into intestinal stem cells. Nat. Rev. Gastroenterol. Hepatol. 16, 19–34.
Gesing, J., Scheuermann, K., Wagner, I.V., Löffler, D., Friebe, D., Kiess, W., Schuster, V., Körner, A., 2017. NAMPT serum levels are selectively elevated in acute infectious disease and in acute relapse of chronic inflammatory diseases in children. PLoS One 12, e0183027.
Han, X., Uchiyama, T., Sappington, P.L., Yaguchi, A., Yang, R., Fink, M.P., Delude, R.L., 2003. NAD^+ ameliorates inflammation-induced epithelial barrier dysfunction in cultured enterocytes and mouse ileal mucosa. J. Pharmacol. Exp. Therapeut. 307, 443–449.
Heer, C.D., Sanderson, D.J., Voth, L.S., Alhammad, Y.M.O., Schmidt, M.S., Trammell, S. A.J., Perlman, S., Cohen, M.S., Fehr, A.R., Brenner, C., 2020. Coronavirus infection and PARP expression dysregulate the NAD metabolome: an actionable component of innate immunity. J. Biol. Chem. 295, 17986–17996.
Holloway, E.M., Czerwinski, M., Tsai, Y.H., Wu, J.H., Wu, A., Childs, C.J., Walton, K.D., Sweet, C.W., Yu, Q., Glass, I., Treutlein, B., Camp, J.G., Spence, J.R., 2021. Mapping development of the human intestinal niche at single-cell resolution. cell. Stem Cell. 28, 568–580 e4.
Hwang, D., Jo, H., Ma, S.H., Lim, Y.H., 2018. Oxyresveratrol stimulates mucin production in an NAD^+-dependent manner in human intestinal goblet cells. Food Chem. Toxicol. 118, 880–888.
Jia, S.H., Li, Y., Parodo, J., Kapus, A., Fan, L., Rotstein, O.D., Marshall, J.C., 2004. Pre-B cell colony-enhancing factor inhibits neutrophil apoptosis in experimental inflammation and clinical sepsis. J. Clin. Invest. 113, 1318–1327.
Kong, W.G., Li, S.S., Chen, X.X., Huang, Y.Q., Tang, Y., Wu, Z.X., 2017. A study of the damage of the intestinal mucosa barrier structure and function of *Ctenopharyngodon idella* with *Aeromonas hydrophila*. Fish Physiol. Biochem. 43, 1223–1235.
Li, Y., Ma, X., Li, J., Yang, L., Zhao, X., Qi, X., Zhang, X., Zhou, Q., Shi, W., 2019. Corneal denervation causes epithelial apoptosis through inhibiting NAD^+ biosynthesis. Invest. Ophthalmol. Vis. Sci. 60, 3538–3546.
Liu, Q., Liu, J., Liang, Q., Qi, Y., Tao, M., Zhang, C., Qin, Q., Zhao, R., Chen, B., Liu, S., 2019a. A hybrid lineage derived from hybridization of *Carassius cuvieri* and *Carassius auratus* red var. and a new type of improved fish obtained by back-crossing. Aquaculture 505, 173–182.
Liu, Q., Qi, Y., Liang, Q., Song, J., Liu, J., Li, W., Shu, Y., Tao, M., Zhang, C., Qin, Q., Wang, J., Liu, S., 2019b. Targeted disruption of tyrosinase causes melanin reduction in *Carassius auratus cuvieri* and its hybrid progeny. Sci. China Life Sci. 62, 1194–1202.
Liu, Q., Qi, Y., Liang, Q., Xu, X., Hu, F., Wang, J., Xiao, J., Wang, S., Li, W., Tao, M., Qin, Q., Zhao, R., Yao, Z., Liu, S., 2018. The chimeric genes in the hybrid lineage of *Carassius auratus cuvieri* (♀)×*Carassius auratus* red var. (♂). Sci. China Life Sci. 61, 1079–1089.
Luo, S.W., Xiong, N.X., Luo, Z.Y., Fan, L.F., Luo, K.K., Mao, Z.W., Liu, S.J., Wu, C., Hu, F. Z., Wang, S., Wen, M., 2021. A novel NK-lysin in hybrid crucian carp can exhibit cytotoxic activity in fish cells and confer protection against *Aeromonas hydrophila* infection in comparison with *Carassius cuvieri* and *Carassius auratus* red var. Fish Shellfish Immunol. 116, 1–11.
Luo, Z., Li, M., Wu, Y., Meng, Z., Martin, L., Zhang, L., Ogunrinde, E., Zhou, Z., Qin, S., Wan, Z., Westerink, M.A.J., Warth, S., Liu, H., Jin, P., Stroncek, D., Li, Q.Z., Wang, E., Wu, X., Heath, S.L., Li, Z., Alekseyenko, A.V., Jiang, W., 2019. Systemic translocation of *Staphylococcus* drives autoantibody production in HIV disease. Microbiome 7, 25.
Ma, S., Yeom, J., Lim, Y.H., 2020. Exogenous NAD^+ stimulates MUC2 expression in LS 174T goblet cells via the PLC-Delta/PTGES/PKC-Delta/ERK/CREB signaling pathway. Biomolecules 10, 580.
Malam, Z., Parodo, J., Waheed, F., Szaszi, K., Kapus, A., Marshall, J.C., 2011. Pre-B cell colony-enhancing factor (PBEF/Nampt/visfatin) primes neutrophils for augmented respiratory burst activity through partial assembly of the NADPH oxidase. J. Immunol. 186, 6474–6484.
Moschen, A.R., Kaser, A., Enrich, B., Mosheimer, B., Theurl, M., Niederegger, H., Tilg, H., 2007. Visfatin, an adipocytokine with proinflammatory and immunomodulating properties. J. Immunol. 178, 1748–1758.
Ogunrinde, E., Zhou, Z., Luo, Z., Alekseyenko, A., Li, Q.Z., Macedo, D., Kamen, D.L., Oates, J.C., Gilkeson, G.S., Jiang, W., 2019. A link between plasma microbial translocation, microbiome, and autoantibody development in first-degree relatives of systemic lupus erythematosus patients. Arthritis Rheum. 71, 1858–1868.
R Moschen, A., R Gerner, R., Tilg, H., 2010. Pre-B cell colony enhancing factor/NAMPT/visfatin in inflammation and obesity-related disorders. Curr. Pharmaceut. Des. 16, 1913–1920.
Ratnayake, D., Nguyen, P.D., Rossello, F.J., Wimmer, V.C., Tan, J.L., Galvis, L.A., Julier, Z., Wood, A.J., Boudier, T., Isiaku, A.I., Berger, S., Oorschot, V., Sonntag, C., Rogers, K.L., Marcelle, C., Lieschke, G.J., Martino, M.M., Bakkers, J., Currie, P.D., 2021. Macrophages provide a transient muscle stem cell niche via NAMPT secretion. Nature 591, 281–287.
Schirmer, H., Pereira, T.C., Rico, E.P., Rosemberg, D.B., Bonan, C.D., Bogo, M.R., Souto, A.A., 2012. Modulatory effect of resveratrol on SIRT1, SIRT3, SIRT4, PGC1α and NAMPT gene expression profiles in wild-type adult zebrafish liver. Mol. Biol. Rep. 39, 3281–3289.
Sugimoto, K., Ogawa, A., Mizoguchi, E., Shimomura, Y., Andoh, A., Bhan, A.K., Blumberg, R.S., Xavier, R.J., Mizoguchi, A., 2008. IL-22 ameliorates intestinal inflammation in a mouse model of ulcerative colitis. J. Clin. Invest. 118, 534–544.
Sultani, G., Samsudeen, A.F., Osborne, B., Turner, N., 2017. NAD^+: a key metabolic regulator with great therapeutic potential. J. Neuroendocrinol. 29, e12508.
Travelli, C., Colombo, G., Mola, S., Genazzani, A.A., Porta, C., 2018. NAMPT: a pleiotropic modulator of monocytes and macrophages. Pharmacol. Res. 135, 25–36.
Zhang, L.Q., Van Haandel, L., Xiong, M., Huang, P., Heruth, D.P., Bi, C., Gaedigk, R., Jiang, X., Li, D.Y., Wyckoff, G., Grigoryev, D.N., Gao, L., Li, L., Wu, M., Leeder, J.S., Ye, S.Q., 2017. Metabolic and molecular insights into an essential role of nicotinamide phosphoribosyltransferase. Cell Death Dis. 23, e2705.
Zhao, X.L., Jin, Z.H., Di, G.L., Li, L., Kong, X.H., 2019. Molecular characteristics, pathogenicity and medication regimen of *Aeromonas hydrophila* isolated from common carp (*Cyprinus carpio L.*). J. Vet. Med. Sci. 81, 1769–1775.
Zhou, Z., Feng, C., Liu, X., Liu, S., 2020. 3nLcn2, a teleost lipocalin 2 that possesses antimicrobial activity and inhibits bacterial infection in triploid crucian carp. Fish Shellfish Immunol. 102, 47–55.
Zhou, Z., Guille, C., Ogunrinde, E., Liu, R., Luo, Z., Powell, A., Jiang, W., 2018. Increased systemic microbial translocation is associated with depression during early pregnancy. J. Psychiatr. Res. 97, 54–57.
Zhou, Z.J., Sun, L., 2015. CsCTL1, a teleost C-type lectin that promotes antibacterial and antiviral immune defense in a manner that depends on the conserved EPN motif. Dev. Comp. Immunol. 50, 69–77.
Zhou, Z.J., Sun, L., 2016. *Edwardsiella tarda*-induced inhibition of apoptosis: a strategy for intracellular survival. Front. Cell. Infect. Microbiol. 6, 76.
Zihni, C., Mills, C., Matter, K., Balda, M.S., 2016. Tight junctions: from simple barriers to multifunctional molecular gates. Nat. Rev. Mol. Cell Biol. 17, 564–580.